Antiviral Research 247 (2026) 106342

Contents lists available at ScienceDirect

Antiviral Research

journal homepage: www.elsevier.com/locate/antiviral

Therapeutic intranasal delivery of NanoSTING provides broad protection against seasonal and highly pathogenic influenza strains

Ankita Leekha [a,1], Kate Reichel [a,1], Brett Hurst [b], Navin Varadarajan [a,*]

[a] Department of Chemical and Biomolecular Engineering, University of Houston, Houston, TX, USA
[b] Institute for Antiviral Research, Utah State University, Logan, UT, USA

ARTICLE INFO

Keywords:
NanoSTING
Nanoparticles
Liposomes
Treatment
Influenza

ABSTRACT

Influenza is a major global threat due to several factors, including great zoonotic potential, ongoing antigenic drift, limited effectiveness of current vaccines, and the emergence of drug-resistant viral strains. Broad-spectrum therapeutic regimens that can treat vulnerable populations, enable faster resolution of symptoms, and decrease fatality rates are a long-sought objective for influenza. Here, we report the development of NanoSTING, a liposomally encapsulated STING agonist (cGAMP), as a single-dose intranasal treatment of influenza. We demonstrate that NanoSTING is stable under simple refrigeration conditions, with no loss of encapsulated cGAMP, for up to a year. A single dose of NanoSTING administered intranasally induced robust type I interferon responses in the nasal and lung tissue of mice without observable toxicity. In mouse challenge models of influenza A (H1N1 or highly pathogenic H5N1) and influenza B, NanoSTING provided therapeutic protection at least as effective as ten doses of oseltamivir. NanoSTING demonstrated therapeutic efficacy even when administered 48–72 h post-infection. Furthermore, NanoSTING maintained its activity in aged and immunocompromised mice, as evidenced by the robust induction of interferon responses in nasal tissues, highlighting its potential for use in vulnerable individuals. These attributes of NanoSTING support its potential use as a promising host-directed antiviral with a large therapeutic window and broad-spectrum efficacy.

1. Introduction

Influenza viruses continue to pose a significant global health burden. These viruses are responsible for seasonal epidemics and pose a continual threat of pandemics due to their high mutation rates and potential for zoonotic transmission (Petrova and Russell, 2018). According to the World Health Organization (WHO), seasonal influenza leads to an estimated 290,000–650,000 deaths annually from respiratory-related illnesses alone (Organization). Despite global surveillance and vaccination efforts, influenza continues to cause widespread morbidity and mortality, particularly among vulnerable populations, including the elderly, immunocompromised individuals, and young children (Organization; Krammer et al., 2018).

Current influenza control strategies primarily rely on annual intramuscular vaccination and antiviral medications such as oseltamivir. These approaches, however, suffer from key limitations. The effectiveness of seasonal vaccines can vary significantly due to antigenic drift, often falling below 50 % efficacy, and their capacity to generate mucosal immunity, which is essential for combating respiratory pathogens, is limited (Batool et al., 2023; Osterholm et al., 2012). The limited effectiveness, in turn, erodes confidence in the vaccine, leading to lower annual vaccination rates and consequently higher infections (Andrews et al., 2011; Axelsen et al., 2014). Furthermore, the adaptive immune response elicited by vaccination is also less efficacious in vulnerable populations such as the elderly (Peteranderl et al., 2016). Antivirals offer a complementary approach, as they can be administered after signs of infection or as prophylaxis following close contact with an infected individual. The effectiveness of antivirals, such as oseltamivir, is, however, constrained by the emergence of resistant viral strains, narrow therapeutic windows, the need for persistent treatment with multiple doses, and modest efficacy when administered as a therapeutic (Batool et al., 2023; Osterholm et al., 2012; Hurt and Kelly, 2016). Emerging preclinical data indicate that certain highly pathogenic H5N1 isolates carrying neuraminidase mutations, such as I117T, exhibit reduced susceptibility to oseltamivir (Kode et al., 2019). Together, these limitations underscore an urgent need for novel, broadly effective therapeutic

* Corresponding author. Department of Chemical and Biomolecular Engineering, University of Houston Houston, Texas TX, 77204, USA.
E-mail address: varadar@central.uh.edu (N. Varadarajan).
[1] These authors contributed equally.

https://doi.org/10.1016/j.antiviral.2026.106342
Received 22 October 2025; Received in revised form 14 December 2025; Accepted 6 January 2026
Available online 15 January 2026

strategies.

Interferons, both type I and III, impact the progression of disease in influenza. Type I interferons (IFNs), such as IFN-α and IFN-β, play a crucial role in combating influenza by inducing interferon-stimulated genes (ISGs) that inhibit viral replication and activate the JAK-STAT signaling pathway to enhance antiviral immunity (Wu and Metcalf, 2020; Killip et al., 2015). However, excessive IFN signaling can cause severe inflammation and lung damage through mechanisms like TRAIL-DR5 interactions, particularly in certain influenza strains or vulnerable hosts (Davidson et al., 2014; Du et al., 2020). Recombinant IFN-α has been used for the treatment of cancer and chronic viral infections since 1986, but its use in influenza is limited due to both antiviral and immunopathogenic effects (Wu and Metcalf, 2020). Prophylactic administration of type I IFNs, such as low-dose oral IFN-α, can reduce influenza severity and replication, while post-infection treatment is often ineffective and may exacerbate inflammation (Wu and Metcalf, 2020; Du et al., 2020). Type III IFNs (IFN-λ) provide a rapid, non-inflammatory response to limit viral spread in the upper airways and might be the key to triggering T-cell immunity, but their integrated efficacy and toxicity are underexplored (Wu and Metcalf, 2020; Hemann et al., 2019). Collectively, these studies highlight the need for precise control of IFN signaling to optimize outcomes in influenza infection (Wu and Metcalf, 2020; Li et al., 2012).

The stimulator of interferon genes (STING) pathway has emerged as a promising avenue for enhancing antiviral immunity. STING is a central regulator of innate immune responses to cytosolic DNA and RNA, inducing the expression of type I interferons (e.g., *Ifnb*) and interferon-stimulated chemokines such as *Cxcl10*, which are critical for antiviral defense (Garcia et al., 2023; Ahn and Barber, 2019; Ishikawa et al., 2009). Cyclic GMP-AMP (cGAMP), an endogenous second messenger synthesized by cGAS in response to cytosolic DNA, is a potent STING agonist (Ablasser et al., 2013). However, its clinical application is limited by poor cellular uptake and rapid degradation (Yu et al., 2024; Li et al., 2014). Nanoparticle-based delivery systems, particularly liposomes, offer a promising strategy to overcome these challenges by enhancing cellular targeting, protecting the cargo from degradation, and facilitating mucosal delivery (Ablasser et al., 2013; Calzas and Chevalier, 2019; Liu et al., 2022). We have previously demonstrated that liposomally encapsulated cGAMP (NanoSTING) delivered intranasally can elicit robust innate immune responses and protect against respiratory viruses by targeting key immune cells in the nasal and lung compartments; (Leekha et al., 2024c).

In this current study, we demonstrate the use of NanoSTING as a therapeutic against a broader spectrum of influenza viruses (both A & B strains). We show several favorable properties of NanoSTING as a candidate therapeutic for human translation: (1) excellent stability for up to a year, (2) broad-spectrum activity against multiple strains of influenza, (3) therapeutic window of 48–72 h after challenge with just a single dose of treatment, and (4) uncompromised activation of innate immunity in vulnerable populations.

2. Results

2.1. NanoSTING activates type I interferon responses in nasal and lung tissue without inducing toxicity

NanoSTING is a liposomal formulation that encapsulates the endogenous STING agonist, cGAMP (Fig. 1A) (Allen and Cullis, 2013; Gajewski and Corrales, 2015). cGAMP can naturally be transported across cell membranes using several transporters, including SLC19A1 and LRRC8A transporters, which play a crucial role in its uptake primarily into immune cells and activation of the STING pathway (Kumar et al., 2023; Ritchie et al., 2019; Blest and Chauveau, 2023). Our prior work demonstrated that upon liposomal encapsulation to yield NanoSTING, cGAMP is delivered primarily to epithelial cells and myeloid cells within the nasal compartment (Leekha et al., 2024a).

To assess the long-term stability of NanoSTING at 4 °C, we measured the particle diameter and zeta potential at various time points over 12 months. NanoSTING maintained a consistent particle size (120 ± 30 nm) with a low polydispersity index (PDI <0.1) throughout all time points tested (Fig. 1B–Supplementary Table 1). The zeta potential remained unchanged during this same period of observation (Fig. 1C). We confirmed these DLS results independently using NanoSight nanoparticle tracking analysis (NTA) (Supplementary Fig. 1, Supplementary Table 2); we were also able to visually confirm the shape and size of the NanoSTING liposomes using NTA (Supplementary Video 1). These findings confirm that NanoSTING maintains its physicochemical characteristics with simple refrigeration. We quantified the amount of encapsulated cGAMP using HPLC, and these results showed no change in the amount of cGAMP over time, supporting NanoSTING's structural integrity and indicating minimal drug leakage for up to a year (Fig. 1D).

One of the advantages of liposomal encapsulation is that it reduces the effective dose of cGAMP necessary for efficacy. We compared the ability of NanoSTING and cGAMP to activate the STING pathway in *BALB/c* mice by measuring the expression of key effector cytokines, C–X–C motif chemokine ligand 10 (*Cxcl10*) and interferon beta (*Ifnb1*) following intranasal administration, as we have published previously (Leekha et al., 2024a). Mice were divided into groups and administered a single intranasal dose of either PBS (Control), NanoSTING (0.2 mg/kg encapsulated cGAMP), or cGAMP (2 mg/kg), and euthanized 24 h after administration for collection of nasal tissue and lungs (Fig. 1E). In the nasal tissue, NanoSTING-mediated activation of *Ifnb1* (1200 ± 500 fold compared to PBS 1.1 ± 0.3) was comparable to cGAMP-mediated activation of *Ifnb1* (600 ± 100 fold compared to PBS) [Fig. 1F]. Upregulation of *Cxcl10* followed a similar pattern with both treatments showing no significant differences (Fig. 1F). These findings demonstrate that NanoSTING achieves comparable activation of the STING pathway at one-tenth the dose of free cGAMP.

To validate our initial observations in the nasal compartment and to explore whether STING activation extends to lungs, we repeated the experiment, isolated nasal tissue for confirmation, and evaluated lung tissue in parallel. We assessed the upregulation of *Ifnb1* and *Cxcl10* gene expression in both nasal tissue and lungs. Consistent with intranasal delivery, the magnitude of activation in the nasal compartment was again higher and more uniform across the animals (*Ifnb1*, 2800 ± 800 fold compared to PBS, 1.9 ± 0.9) whereas the activation in the lung was 10-fold lower and more heterogenous across the animals (*Ifnb1*, 100 ± 100 fold compared to PBS, 1.6 ± 0.7) [Fig. 1G–H]. To evaluate safety in the lung, we conducted hematoxylin and eosin (H&E) staining to assess the safety of NanoSTING following intranasal administration in lung tissues. Mice treated with NanoSTING (0.2 mg/kg) displayed normal lung architecture, with no evidence of inflammation, confirming its safety (Fig. 1I). Similarly, mice treated with cGAMP (2 mg/kg) showed no histological abnormalities. Collectively, these findings confirm that NanoSTING activates innate immune responses without inducing toxicity (Fig. 1I).

2.2. NanoSTING reduces disease severity more effectively in influenza A infection compared with oseltamivir

We assessed the protective effects of NanoSTING against aerosolized Influenza A virus in a murine model. *BALB/c* mice were challenged with $1 \times 10^{4.3}$ $CCID_{50}$ of Influenza A/California/04/2009 (H1N1dpm) strain and treated with either NanoSTING (single intranasal dose at 24 h post infection (hpi), oseltamivir (30 mg/kg/day for five days, starting at 12 hpi), or a placebo (PBS) [Fig. 2A]). The results demonstrated that the placebo group experienced a severe decline in body weight (mean peak weight loss: 29.6 %), indicative of significant disease progression. In contrast, the oseltamivir-treated groups exhibited reduced weight loss (mean peak weight loss: 26.9 ± 0.8 %), with NanoSTING-treated mice showing a significantly lower weight loss (mean peak weight loss: 19 ± 2 %) (Fig. 2B). Notably, the NanoSTING-treated animals showed faster

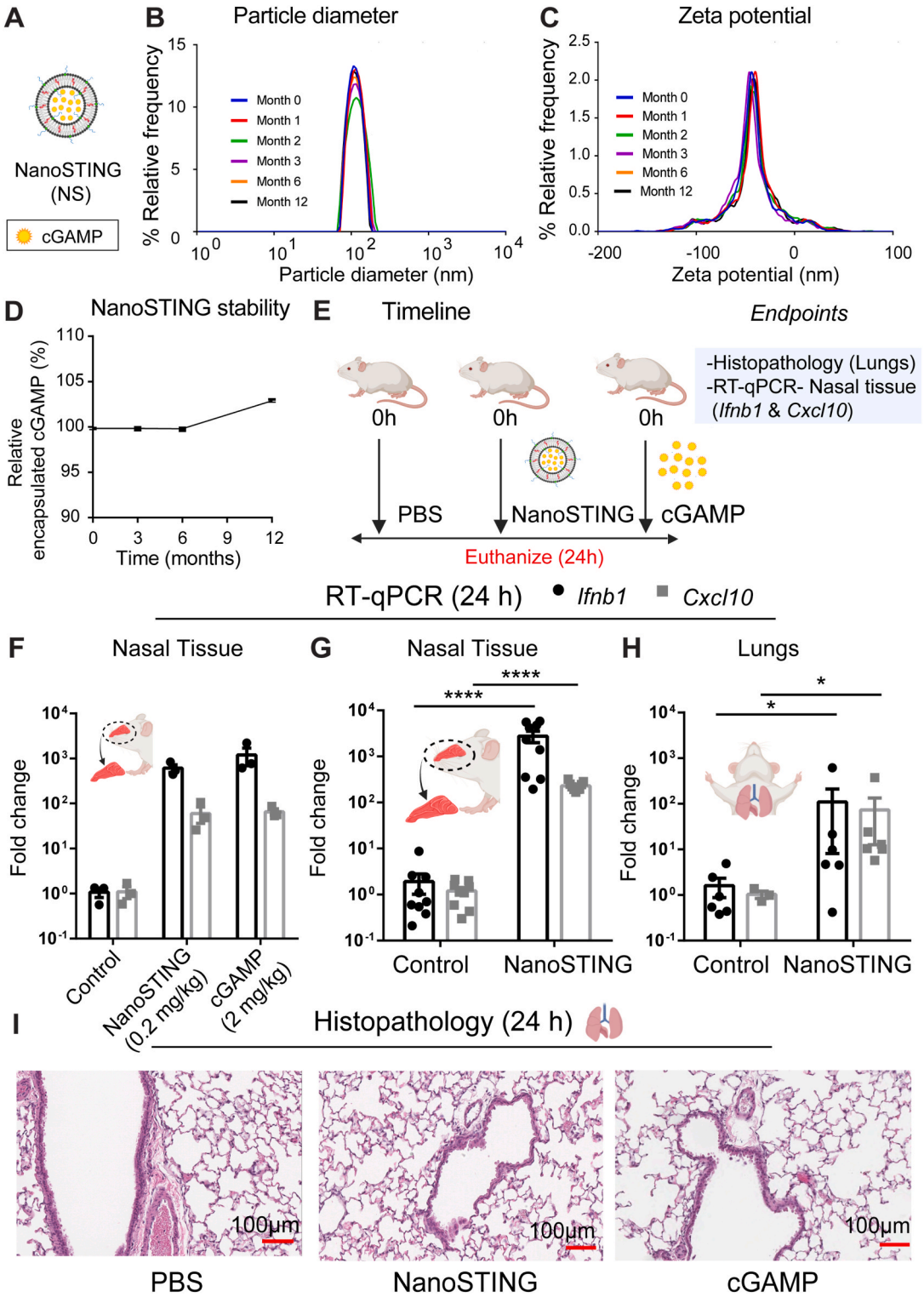

Fig. 1. Stability and efficacy of NanoSTING formulations.
A) Schematic of NanoSTING (NS), a liposomal formulation encapsulating cGAMP, a natural STING agonist.
(B) Particle size distribution of NanoSTING measured over a 12-month period using dynamic light scattering.
(C) Zeta potential measurements of NanoSTING over a 12-month period.
(D) HPLC based quantification of encapsulated cGAMP in NanoSTING over a 12-month period.
(E) Schematic of RT-qPCR experimental design. Mice were intranasally administered PBS, NanoSTING (0.2 mg/kg), or free cGAMP (2 mg/kg), and euthanized after 24 h for tissue collection (nasal tissue and lungs).
(F) RT-qPCR analysis of *Ifnb1* (black bars) and *Cxcl10* (gray bars) expression in nasal tissues from mice treated with PBS, NanoSTING, or cGAMP (n = 3). (G) Independent replication in a second cohort of mice showing robust *Ifnb1* and *Cxcl10* induction in nasal tissues following NanoSTING administration (n = 9).
(H) RT-qPCR analysis of *Ifnb1* and *Cxcl10* expression in lung tissues after NanoSTING treatment (n = 3–6 across groups).
(I) Representative H & E-stained lung sections from mice 24 h after treatment with PBS, NanoSTING, or cGAMP (scale bar = 100 μm), Magnification 20x.

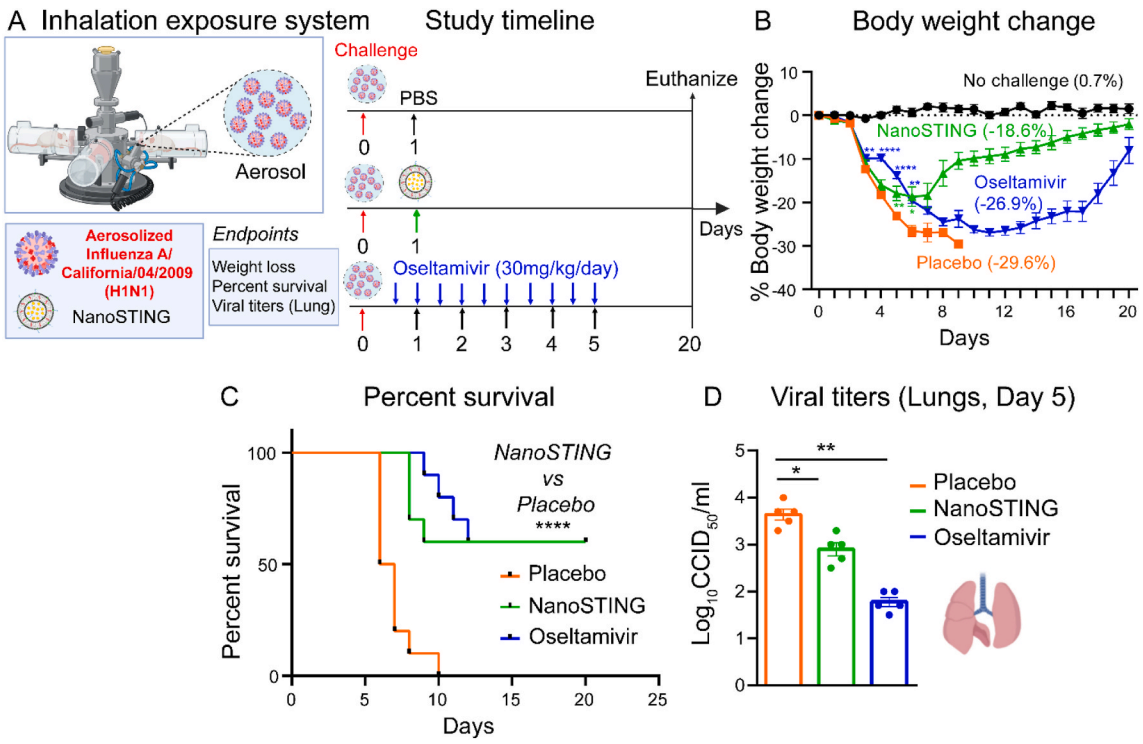

Fig. 2. Single-dose therapeutic administration of NanoSTING offers protection against Influenza A comparable to 10 doses of oseltamivir
(A) Schematic of experimental design. *BALB/c* mice (n = 10/group) were challenged with an aerosolized dose of $1 \times 10^{4.3}$ $CCID_{50}$ of Influenza A/California/04/2009 (H1N1dpm) virus. Following the challenge, groups of mice received the following treatments: a single dose of NanoSTING (0.2 mg/kg), oseltamivir administered at 30 mg/kg/day (with the first dose given 4 h post-infection, followed by 9 subsequent doses every 12 h), or a placebo treatment (PBS). Blood samples were taken on day 0, and treatments were administered as indicated. Mice were euthanized at the end of the study (day 20) to assess endpoints, including percent survival and weight loss.
(B) Change in body weight over time for different treatment groups. Asterisks indicate significance compared to the placebo-treated animals at each time point. Mann–Whitney *U* test ****$p < 0.0001$; ***$p < 0.001$; **$p < 0.01$; *$p < 0.05$. The exact p-values comparing the NanoSTING group to the Placebo group are Day 5: $p = 7e{-}3$ and Day 6: $p = 2e{-}2$. Additionally, for the Oseltamivir-treated group compared with Placebo, the significant p-values are Day 3: $p = 3e{-}3$, Day 4: $p = 1e{-}4$, Day 5: $p = 1e{-}4$, and Day 6: $p = 2e{-}3$.
(C) Kaplan-Meier survival curves showing percent survival of mice in the different treatment groups. p-values were calculated using the log-rank (Mantel–Cox) test.
(D) Viral titers in lung tissues at day 5, presented as Log_{10} $CCID_{50}$/mL. Statistical significance is indicated by *$p < 0.05$ and **$p < 0.01$.

recovery from weight loss compared to oseltamivir. Treatment with either NanoSTING or oseltamivir significantly improved survival of mice compared to the placebo treated mice (Fig. 2C). We evaluated viral titers in the lung homogenates; the viral titers were significantly lower in both NanoSTING and oseltamivir-treated groups compared to the placebo group, indicating more rapid viral clearance (Fig. 2D). Statistical comparison confirmed that viral titers in the oseltamivir-treated group were significantly lower than those in the single-dose NanoSTING group ($p = 0.0079$, **), although both treatments resulted in substantial protection compared to placebo. Notably, while receiving only a single intranasal dose, NanoSTING provided recovery at a level similar to multi-dose oseltamivir, enabling survival from lethal influenza challenge.

2.3. *NanoSTING reduces disease severity more effectively in influenza B infection compared with oseltamivir*

To evaluate therapeutic efficacy against influenza B, mice were challenged with $1 \times 10^{4.3}$ $CCID_{50}$ of Influenza B strain B/Brisbane/60/2008 (Victoria lineage) on Day 0 and NanoSTING was administered intranasally 24 hpi, while oseltamivir (30 mg/kg/day) was given twice daily for five days starting at 12 hpi (Fig. 3A). In the placebo group, mean peak body weight loss of −28.8 % was observed by day 7. In contrast, the oseltamivir-treated group (with a mean peak weight loss of -26 ± 2 %) experienced less severe weight loss and increased survival (Fig. 3B and C). Similar to the results with influenza A infected animals, the NanoSTING treated animals had less severe weight loss (mean peak weight loss of -11 ± 3 %) and a more rapid recovery in body weight compared to both oseltamivir and placebo groups (Fig. 3B). While the untreated animals did not survive, treatment with either oseltamivir or NanoSTING significantly improved survival (Fig. 3C). Collectively, these findings suggest that NanoSTING is effective in mitigating loss in body weight and promoting recovery, better than oseltamivir, further strengthening its translational potential.

2.4. *NanoSTING induces potent immune response in immunocompromised and aged mouse models*

Given the increased susceptibility of immunocompromised and aged populations to severe influenza outcomes, we aimed to evaluate the immunostimulatory effects of NanoSTING in these models. Lymphopenia, either due to natural reasons like autoimmune diseases or induced due to medications (e.g., chemotherapies for cancer), increases the likelihood of infections and is associated with high risk of mortality among adults (Zidar et al., 2019). Accordingly, we evaluated the ability of NanoSTING to activate the innate immune system in lymphodepleted animals by using three groups of animals: (1) mice receiving cyclophosphamide (CFX) alone, (2) mice receiving only a single intranasal dose of NanoSTING (0.2 mg/kg), and (3) mice that were pre-treated with CFX and, 48 h later, treated with a single intranasal dose of NanoSTING (Fig. 4A). Quantification of *Ifnb1* and *Cxcl10* in the nasal tissue using RT-qPCR confirmed that pre-treatment with CFX had no significant impact on the ability of NanoSTING to upregulate either *Ifnb1*

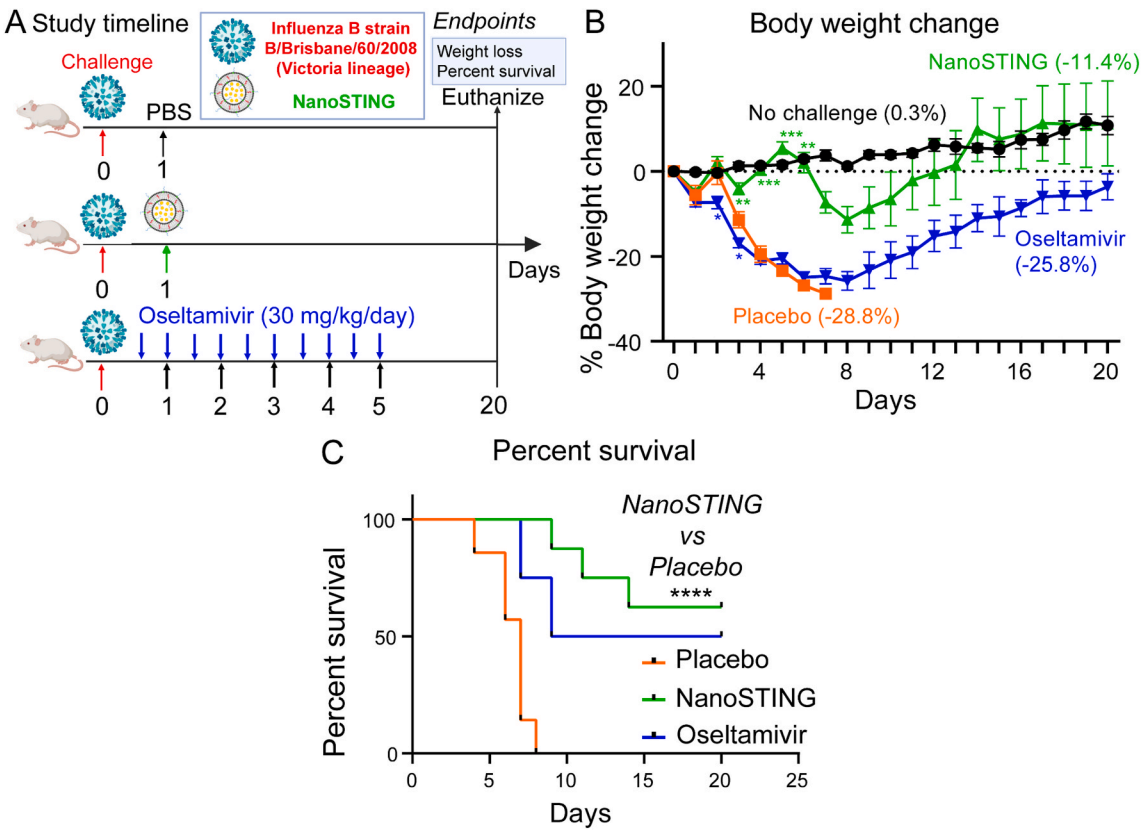

Fig. 3. Single-dose therapeutic administration of NanoSTING offers enhanced protection against Influenza B compared with oseltamivir
(A) Study timeline. *BALB/c* mice (n = 6–8 across groups) were challenged with an aerosolized dose of $1 \times 10^{4.3}$ $CCID_{50}$ of Influenza B strain B/Brisbane/60/2008 (Victoria lineage) virus. The treatment groups included intranasal NanoSTING (0.2 mg/kg), oral oseltamivir administered at 30 mg/kg/day (with the first dose given 4 h post-infection, followed by 9 additional doses every 12 h over 5 days), or placebo (PBS). Mice were euthanized on day 20 to assess endpoints such as survival and body weight change.
(B) Change in body weight over time for different treatment groups. Asterisks indicate significance compared to the placebo-treated animals at each time point. Mann–Whitney *U* test ****$p < 0.0001$; ***$p < 0.001$; **$p < 0.01$; *$p < 0.05$. The exact p-values comparing the NanoSTING group to the Placebo group are Day 3: $p =$ 6e−3, Day 4: $p =$ 3e−4, Day 5: $p =$ 7e−4, and Day 6: $p =$ 4e−3. Additionally, for the Oseltamivir-treated group compared with Placebo, the significant p-values are Day 2: $p =$ 1e−2 and Day 3: $p =$ 1e−2.
(C) Kaplan–Meier survival curves for mice in each treatment group. *p*-values were calculated using the log-rank (Mantel–Cox) test.

(3000 ± 2000 fold for NanoSTING treated mice vs 4500 ± 1000 fold for CFX + NanoSTING treated mice) or *Cxcl10* (110 ± 30 fold for NanoSTING treated mice vs 120 ± 20 fold CFX + NanoSTING treated mice) [Fig. 4B]. Hence, NanoSTING retains innate immunostimulatory activity under cyclophosphamide-induced lymphodepletion, supporting its use in vulnerable hosts.

Corticosteroids have become indispensable tools for controlling inflammation in modern medicine and are used to treat a wide range of inflammatory disorders, including chronic diseases such as rheumatoid arthritis, asthma, and inflammatory bowel disease. Since corticosteroids are also immunosuppressive, we tested whether the treatment with a commonly used corticosteroid, dexamethasone, interferes with NanoSTING. We treated a groups of mice with either: (1) Dexamethasone (DX) alone, (2) single-dose intranasal NanoSTING (0.2 mg/kg), or (3) treatment with DX and 24 h later treated mice with a single intranasal dose of NanoSTING (Fig. 4C). Quantification of *Ifnb1* and *Cxcl10* in the nasal tissue using qPCR confirmed that pre-treatment with DX had no significant impact on the ability of NanoSTING to upregulate either *Ifnb1* (1300 ± 300 fold for NanoSTING treated mice vs 1600 ± 300 fold for DX + NanoSTING treated mice) or *Cxcl10* (370 ± 90 fold for NanoSTING treated mice vs 400 ± 200 fold for DX + NanoSTING treated mice) [Fig. 4D].

Older adults (>65 years old) are at higher risk of developing serious complications from influenza infections compared to younger adults. One of the primary reasons for this risk is that the adaptive immune system weakens with advanced age. We sought to determine whether NanoSTING-mediated activation of the innate immune system is preserved in aged mice, serving as a surrogate for elderly humans. We treated groups of old mice (18–22 months) intranasally with low dose of NanoSTING (0.1 mg/kg) to determine their efficacy and compared their responses with those of the young mice (2 months) (Fig. 4E). RT-qPCR confirmed that the upregulation of *Ifnb1* (100 ± 20 fold for aged mice vs 90 ± 40 fold for young mice) or *Cxcl10* (70 ± 20 fold for aged mice vs 50 ± 20 fold for young mice) in the nasal compartment was no different when comparing aged to young mice, indicating that age did not impair NanoSTING's ability to activate these key antiviral pathways in nasal tissue (Fig. 4F). Taken together, these results demonstrate that NanoSTING-mediated activation of the innate immune system is largely preserved in animal models of the vulnerable populations.

2.5. *NanoSTING attenuates H5N1-induced weight loss in mice*

Since 2001, there has been a resurgence of highly pathogenic avian influenza HPAI A(H5N1) virus transmission among birds, and in 2024, human infections were reported (Webby and Uyeki, 2024). We investigated whether NanoSTING could offer protection against HPAI H5N1, which induces significant respiratory illness and weight loss in infected mice. Groups of mice were challenged with H5N1 and treated with a single intranasal dose of NanoSTING as either a pretreatment (24 h before challenge) or post-treatment (24, 48, or 72 hpi). In this animal

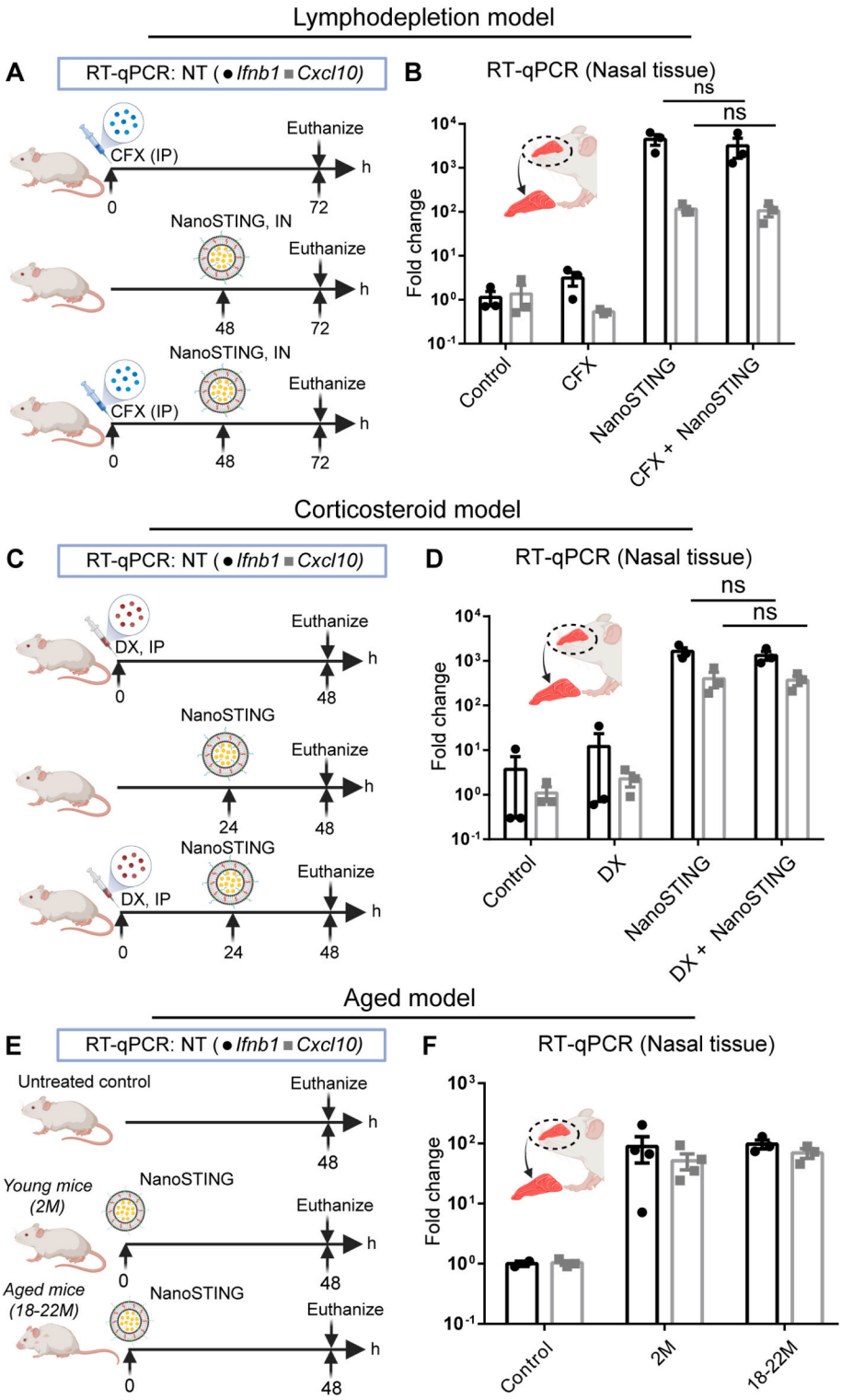

Fig. 4. NanoSTING induces activation of *Ifnb1* and *Cxcl10* in immunocompromised and aged mice models

(A) Schematic of experimental design for RT-qPCR analysis of nasal tissue (NT) to assess *Ifnb1* and *Cxcl10* expression. Mice (n = 3–4/group) were treated with cyclophosphamide (CFX) via intraperitoneal injection (IP) at 0 h, followed by intranasal (IN) administration of NanoSTING (0.2 mg/kg) at 48 h. Mice were euthanized at 72 h for analysis.

(B) RT-qPCR results showing fold change in *Ifnb1* (blue) and *Cxcl10* (red) expression in nasal tissues of different treatment groups.

(C) Schematic of experimental design for RT-qPCR analysis of nasal tissue. Mice (n = 3/group) were treated with dexamethasone (DX, IP) at 0 h, followed by intranasal NanoSTING (0.2 mg/kg) at 24 h. Mice were euthanized at 48 h for analysis.

(D) RT-qPCR results showing fold change in *Ifnb1* and *Cxcl10* expression in nasal tissues of different treatment groups.

(E) Schematic of experimental design to assess the effect of age on RT-qPCR analysis of *Ifnb1* and *Cxcl10* expression. Young *BALB/c* (2 months; n = 4) and aged *B.129* mice (18–22 months; n = 4) were administered NanoSTING (0.1 mg/kg) intranasally and euthanized at 48 h for nasal tissue collection and analysis.

(F) RT-qPCR results showing fold change in *Ifnb1* and *Cxcl10* expression in nasal tissues of young and aged mice compared to the control group.

model, to afford any protection, we had to use oseltamivir at a high dose (75 mg/kg/day) and initiate treatment with oseltamivir 4 hpi, consistent with other published reports (Fig. 5A) (Zheng et al., 2008).

In this HPAI A(H5N1) model, single-dose NanoSTING pretreatment outperformed oseltamivir treatment in preventing weight loss (mean peak weight loss: NanoSTING −3.2 ± 0.8 % vs oseltamivir −5 ± 1 %) and faster recovery, whereas placebo-treated mice exhibited sustained weight loss (Fig. 5B–D). To evaluate the therapeutic window, we initiated NanoSTING treatment 24/48/72 hpi. Surprisingly, treatment at 24 hpi was the least effective at preventing weight loss (mean peak weight loss: 13 ± 2 %), whereas 48 hpi (mean peak weight loss: 12 ± 3 %) and 72 hpi (mean peak weight loss: 11 ± 3 %) showed better protection (Fig. 5E–F). Comparisons of all these groups illustrated that even a single-dose treatment with NanoSTING, given 72 hpi, showed significant improvement in preventing weight loss compared to placebo (Fig. 5G).

The quantification of viral titers in the lungs of NanoSTING-pretreated mice and oseltamivir-treated mice was significantly lower (2 ± 0.4) compared to that of untreated animals (4.9 ± 0.2), confirming that protection was conferred at least partly through reduced viral replication (Fig. 5H). NanoSTING treatment administered at 48 hpi had significantly lower viral titers (2.7 ± 0.3) compared to the placebo 24 hpi group (4.2 ± 0.4) [Fig. 5I]. Notably, the reduction in viral titers with a single dose of NanoSTING initiated 48hpi was comparable to the

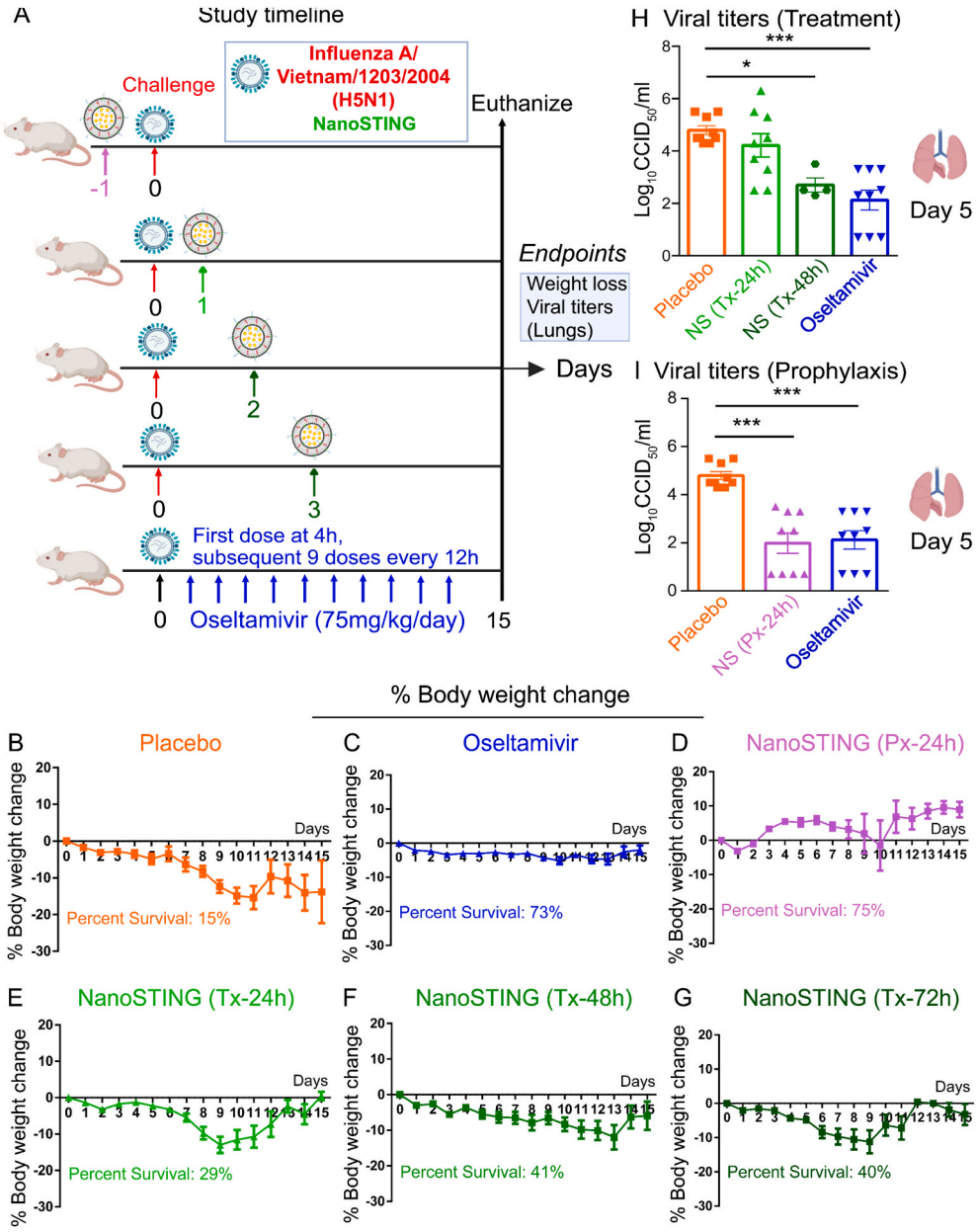

Fig. 5. NanoSTING treatment protects against HPAI A(H5N1) infection.
(A) Schematic of the experimental timeline showing five treatment groups: Mice (n = 14–28 across groups) received either NanoSTING (0.2 mg/kg) prophylactically 24 h before viral challenge (Px-24h), therapeutically at 24-, 48- or 72 h post-challenge (Tx-24h, Tx-48h and Tx-72h), oseltamivir (75 mg/kg/day) starting 4 h post-challenge for 10 doses, PBS (placebo), or no virus challenge (non-challenged controls). (B–G) Body weight change was monitored daily for 15 days across all treatment groups, with the percent survival calculated at day 15. Panel B displays weight trajectories for placebo mice, while Panel C shows weight loss in oseltamivir-treated mice. Panels D–I illustrate weight changes in mice treated with NanoSTING pretreatment (D), and NanoSTING post-treatment at 24 h (E), 48 h (F), or 72 h (G) after challenge.(H–I) Lung viral titers were assessed on Day 5 post-infection. Panel H shows titers from mice receiving NanoSTING post-treatment (Tx-24h, Tx-48h) or oseltamivir. Panel I shows viral titers in mice pretreated with NanoSTING (Px-24h) or oseltamivir.

reduction in viral titers observed with 10 doses of oseltamivir initiated 4 hpi (Fig. 5I).

These results demonstrate that NanoSTING is highly effective in reducing both HPAI (A)H5N1-induced weight loss and viral replication. A single intranasal dose of NanoSTING, whether used as a prophylactic or therapeutic, provided protection at least comparable to multiple doses of oseltamivir. These findings support the potential of NanoSTING as a promising antiviral for both prophylactic and therapeutic use against severe influenza infections, including HPAI (A)H5N1, with a broad window of treatment.

3. Discussion

Efficacious antiviral therapeutics are an essential countermeasure to combat emerging influenza pandemics. Two classes of direct antivirals are currently approved for the treatment of post-exposure prophylaxis of influenza: neuraminidase inhibitors (e.g., oseltamivir and zanamivir) (Cooper et al., 2003) and polymerase inhibitors (e.g., Baloxavir Marboxil) (O'Hanlon and Shaw, 2019). Unfortunately, resistance to both classes of drugs has been reported in humans, underscoring the need to develop broad-spectrum therapeutics (Moscona, 2009; Hayden et al., 2018). Host-targeted therapeutics can activate broad antiviral programs, presenting a complementary strategy for therapeutic protection against viruses.

Oseltamivir is the most widely used clinical antiviral; hence, we used oseltamivir as a comparator in all our challenge studies (Dutkowski, 2010). Oseltamivir is administered as its prodrug, oseltamivir phosphate, which is metabolized into the active form by esterases in the digestive tract, liver, and blood (He et al., 1999). With respect to the pandemic potential influenza viruses, A/H1N1pdm09 and A/H5N1 VN1203/04, preclinical data in mice have shown that improving survival relative to untreated animals requires both a longer duration of treatment (16 doses, twice daily for eight days) and initiating treatment 4h before challenge (Zheng et al., 2008; Yen et al., 2005). These results are consistent with our experimental findings wherein oseltamivir treatment had to be initiated at a high dose (75 mg/kg/day, >3 times higher than the human clinical dose) and within 4 h of challenge to provide protection against A/H5N1 VN1203/04 (Fig. 5). As our results in mice demonstrate, treatment with NanoSTING requires only a single dose and is effective even when administered 48–72 h after viral challenge in mice. From a clinical perspective, oseltamivir, despite being used widely in humans as a therapeutic or post-exposure prophylaxis (within the first 48 h), its efficacy is controversial, with meta studies reporting either no demonstrable benefit or only modest benefit (Gao et al., 2024; Qiu et al., 2015). The advantages of NanoSTING, including the need for only a single dose and a broad therapeutic window, make it an attractive candidate for translation into clinical use. Our previous toxicology studies included detailed histological evaluation of the lungs and other major organs after empty liposome administration and repeated NanoSTING dosing, all of which showed normal tissue architecture even at higher doses. In addition, the toxicology tables in our previous paper, which assessed clinical chemistry, hematology, coagulation, and urinalysis parameters, revealed no abnormalities or evidence of systemic toxicity (Leekha et al., 2024a). Together, these findings support the safety of the formulation and the dosing used in the current study.

Influenza imposes a substantial clinical burden on elderly and immunocompromised populations (Kunisaki and Janoff, 2009). Human studies highlight that adults aged ≥65 years account for 70–85 % of influenza-related deaths and 50–70 % of hospitalizations, driven by chronic comorbidities such as cardiovascular disease, diabetes, and respiratory conditions (Near et al., 2022). Real-world studies have demonstrated that the all-strain effectiveness of the influenza vaccine was directly impacted by age: both young adults (18–64 years, efficacy 36.7 %) and elderly (≥65 years, efficacy 30.6 %) exhibited a significantly lower effectiveness compared with children (<18 years old, efficacy 48.6 %) (Guo et al., 2024). The effectiveness of current vaccines is also strain-specific, with efficacy against influenza A/H3N2 and influenza B Victoria strains being lower than influenza A/H1N1, whereas effectiveness against highly pathogenic strains like influenza A/H5N1 was not evaluable (Guo et al., 2024). The underlying reason for the lower efficacy is best understood from the perspective of immunosenescence: a multifactorial change during aging shaped by chronic inflammation, which manifests as a reduction in the magnitude and duration of antibody and cellular responses against both natural infections and vaccinations (Liu et al., 2023). Similar to the adaptive immune system, the innate immune system also undergoes changes during aging (Lauf et al., 2024). Indeed, the release of cytokines upon activation of innate immune sensors, including STING in human peripheral blood mononuclear cells (PBMCs), shows dampened secretion from older adults compared to young people (Lauf et al., 2024). Consistent with this observation, macrophages from older populations exhibit lower STING expression and consequently a reduced interferon response upon influenza infection (Lauf et al., 2024). Our results in mice demonstrate that NanoSTING-mediated activation of interferons is largely preserved in aged mice and can thus compensate for the suboptimal activation of the STING pathway in these models. Our proof-of-concept data provide promise for testing the efficacy of NanoSTING in larger animal models and eventually elderly humans with the goal of reducing the morbidity/mortality of influenza.

Immunocompromised individuals, such as those with HIV, solid organ or bone marrow transplants, or undergoing chemotherapy, experience prolonged viral shedding (up to 19 days vs. 6.4 days in healthy individuals) and increased rates of severe outcomes, including ICU admissions (8–14 %) and mortality (11–33 % in cancer patients) (Memoli et al., 2014). These groups often exhibit diminished vaccine responses, with antibody titers significantly lower than in healthy controls, underscoring the need for alternative therapeutics (Memoli et al., 2014). Induced immunosuppression, accomplished via the administration of corticosteroids, is used to treat several autoimmune disorders like rheumatoid arthritis. Although the durability and efficacy of influenza vaccines in this cohort are controversial (Kunisaki and Janoff, 2009), the magnitude of humoral responses is lower compared to healthy individuals (Fomin et al., 2006). Our data illustrate that in immunocompromised models pretreated with cyclophosphamide or dexamethasone, NanoSTING elicited significant and rapid upregulation of interferon-stimulated chemokines, suggesting its promise in vulnerable populations.

NanoSTING's liposomal formulation overcomes the inherent limitations of free cGAMP, such as rapid degradation by ectonucleotide pyrophosphatase/phosphodiesterase 1 (ENPP1) and poor cellular transport due to its polar nature and dependence on transporters like SLC19A1 (Luteijn et al., 2019). As we have shown, liposomal encapsulation decreases cGAMP dosing 10-fold, which is similar to the improvements with other liposomal formulations with dexamethasone (Anderson et al., 2010) and chemotherapeutics (Allen and Martin, 2004). The liposomal carrier of NanoSTING enhances cGAMP stability, protects it from rapid clearance, and preferentially targets sentinel cells such as alveolar macrophages and epithelial cells, which are pivotal for orchestrating antiviral immunity (Pöpperl et al., 2025). This targeted delivery enhances the activation of the STING pathway, leading to robust interferon responses that are crucial for combating influenza (Holm et al., 2016). Importantly, the expression of cGAMP transport mechanisms is variable in respiratory tissues (The Human Protein Atlas), which can limit the uptake and distribution of naked cGAMP to target immune cells. As previously published, NanoSTING mediates the delivery of cGAMP to both epithelial cells and alveolar macrophages (Leekha et al., 2024b, 2024c). These mechanistic advantages, coupled with the formulation's stability and single-dose administration, position NanoSTING as a promising candidate for clinical development, where ease of use and long-term shelf stability are critical for broad-spectrum influenza therapeutics.

4. Methods

4.1. Preparation of NanoSTING

The liposomes contained DPPC, DPPG, Cholesterol (Chol), and DPPE-PEG2000 (Avanti Polar lipids) in a molar ratio of 10:1:1:1. To prepare the liposomes, we mixed the lipids in CH_3OH and $CHCl_3$, and we evaporated the mixture at 55 °C using a vacuum rotary evaporator. The resulting lipid thin film was dried overnight in a vacuum chamber to remove residual organic solvent. We hydrated the lipid film by adding a pre-warmed cGAMP (MedChemExpress) solution (3 mg/mL in PBS buffer at pH 7.4). We continuously mixed the hydrated lipids at an elevated temperature of 65 °C for 1 h, and then subjected them to 10 freeze-thaw cycles. Next, we passed the mixture through 0.2-μm followed by 0.1-μm polycarbonate track-etched membranes (Cytiva) using a mini-extruder (Avanti) at 75 °C and measured using dynamic light scattering (DLS) to confirm the targeted size. Finally, we removed the free unencapsulated cGAMP with Amicon Ultrafiltration units (MW cut off 100 kDa). We buffer exchanged the NanoSTING (liposomally encapsulated STINGa) three times using PBS buffer to remove residual cGAMP. We measured the cGAMP concentration in the filtrates with a NanoDrop (Thermo Scientific NanoDrop, 2000c Spectrophotometer) to ensure the unencapsulated cGAMP was lower than 100 ng/μL. We calculated the final concentration of cGAMP in NanoSTING and encapsulation efficiency via HPLC at 260 nm (Shimadzu LC-2050 with PDA). The full HPLC gradient, solvent composition, and flow program used for cGAMP separation are shown in Supplementary Fig. 3. The external calibration curve used to quantify cGAMP by HPLC is provided in Supplementary Fig. 4.

To check the stability, we stored NanoSTING at 4 °C for 1, 2, 3, 6, and 12 months. We measured the average hydrodynamic diameter and zeta potential of liposomal particles using DLS and a zeta sizer on Litesizer 500 (Anton Paar). Visual characterization and NTA measurements of liposomal particles were captured via NanoSight (Malvern NanoSight NS300); a representative video is provided as Supplementary Video 1.

4.2. RT-qPCR for gene expression

In vivo experiments were conducted on *BALB/c* mice to assess the immunostimulatory effect of NanoSTING on the expression of immune-related genes. Mice were randomly assigned to groups and administered either PBS (control), NanoSTING (4 μg), or cGAMP (2 mg/kg). Intranasal administration was performed under 2 % isoflurane anesthesia. Mice were euthanized 24 h post-administration, and nasal turbinates and lung tissues were collected for RNA extraction. We excised mouse nasal turbinate tissues and placed approximately 20 mg of tissue in 2 mL tubes containing 500 μL RNeasy lysis buffer (RLT) and a single stainless-steel bead. Next, we homogenized the tissue using a Tissue Lyser (Qiagen, Hilden, Germany) before extracting total RNA using a RNeasy kit (Qiagen, #74104), following the manufacturer's instructions. Extracted RNA was treated with DNase using a DNA-free DNA removal kit (Invitrogen, #AM1906). Next, 1 μg of total RNA was converted to cDNA using a High-Capacity cDNA reverse transcription kit (Invitrogen, #4368813). We diluted the resultant cDNA to 1:10 before analyzing quantitative real-time polymerase chain reaction (qRT-PCR). We performed qRT-PCR reaction using SsoFast™ EvaGreen® Supermix with Low ROX (Biorad, # 1725211) on an AriaMx Real-time PCR System (Agilent Technologies, Santa Clara, CA). We normalized the results to GAPDH (glyceraldehyde-3-phosphate dehydrogenase). We determined the fold change using the 2-DDCt method, comparing treated mice to naive controls. See Supplementary Table 3 for the primer sequences used in this study.

4.3. Immunocompromised mouse models

Female *BALB/c* mice, aged 6–8 weeks, and B.129 mice, 18–22 months old, were housed under specific pathogen-free conditions with access to food and water ad libitum. All experimental procedures were approved by the Institutional Animal Care and Use Committee (IACUC). Mice were divided into three groups. In the first group, to induce immunosuppression, mice were injected intraperitoneally with cyclophosphamide (CFX, 150 mg/kg) at 0 h, followed by intranasal administration of NanoSTING at 48 h. Mice were euthanized at 72 h for nasal tissue collection. In the second group, dexamethasone (DX, 20 mg/kg) was administered intraperitoneally at 0 h, and NanoSTING was given intranasally at 24 h, with euthanasia and tissue collection at 48 h. The third group consisted of 2-month-old (young *BALB/c* mice) and 18-22-month-old (aged B.129) mice, which received NanoSTING intranasally at 0 h and were euthanized 48 h later. For intranasal administration, mice were lightly anesthetized with isoflurane, and NanoSTING was delivered in a 20 μL volume (10 μL per nostril). Nasal tissues were collected, snap-frozen, and stored at −80 °C. Total RNA was isolated using a commercial kit, and RNA concentration and purity were assessed prior to reverse transcription and quantitative PCR (RT-qPCR) for the analysis of *Ifnb1* and *Cxcl10* expression.

4.4. Viruses

Isolates of Influenza viruses were obtained from BEI Resources (Manassas, VA) and amplified in Madin-Darby canine kidney (MDCK) cells to create working stocks of the virus. Influenza A/California/04/2009 was kindly provided by Elena Govorkova (St. Jude Children's Research Hospital, Memphis, TN) and was adapted to mice by Natalia Ilyushina and colleagues at the same institution. Influenza B/Brisbane/60/2008 (Victoria lineage) and Influenza A/Vietnam/1203/2004 (H5N1) were provided by the Centers for Disease Control and Prevention (CDC, Atlanta, GA). Working stocks of each virus were prepared through two sequential passages of the virus in MDCK cells.

4.5. Biosafety

Studies with Influenza A/California/04/2009 (H1N1pdm) and B/Brisbane/60/2008 viruses were completed within the ABSL-2 space of the Laboratory Animal Research Center (LARC) at USU. Studies with the Influenza A/Vietnam/1203/2004 (H5N1) virus were completed within the ABSL-3+ Select Agent space at the Bioinnovation campus at USU.

4.6. Viral challenge studies in animals

Animals. For influenza virus animal studies, 8-week-old *BALB/c* (Strain code: 028) mice were purchased from Charles River Laboratories and allowed to acclimate for at least 72 h prior to study initiation.

4.7. Influenza challenge and NanoSTING treatment

BALB/c mice were used to assess the protective efficacy of NanoSTING against an aerosolized Influenza A virus and Influenza B challenge. Mice were anesthetized by intraperitoneal injection using a mixture of ketamine/xylazine (50/5 mg/kg) and infected with a 1 x $10^{4.3}$ $CCID_{50}$ dose of influenza virus in a 90 μl volume for mice infected with the Influenza A H1N1pdm or Influenza B viruses, which correlates to a 3 × 50 % lethal dose (LD_{50}). Mice infected with the Influenza A H5N1 virus received a challenge dose of 1 x $10^{\circ.7}$ $CCID_{50}$ in a 90 μl volume, which correlates to a 2 × LD_{50} dose. Mice were first challenged with aerosolized Flu A virus on Day 0 in Study 1 and with Flu B in Study 2. On Day 1, groups of mice were treated either with NanoSTING intranasally or with PBS (control) by intranasal administration after being anesthetized with the same mixture of ketamine/xylazine. In a separate group, oseltamivir (75 mg/kg/day) was administered twice daily via oral gavage from Day 1 to Day 5. Mice were monitored daily for 20 days for changes in body weight, and survival was recorded. On Day 20, surviving animals were euthanized, and blood samples were

collected for analysis. Lung histopathology samples were also collected and stored in 10 % neutral buffered formalin.

4.8. Body weight monitoring

Mice were weighed daily from the start of the experiment (Day 0) until the end of the study (Day 20). The percent change in body weight relative to baseline was calculated. Animals were humanely euthanized if their body weight dropped below 25 % of their baseline weight for two consecutive days. The changes in body weight across the different treatment groups (NanoSTING, Oseltamivir, PBS, and Placebo) over time were recorded. Daily body-weight changes for unchallenged control mice are shown in Supplementary Fig. 5.

4.9. Survival monitoring

Mice were observed daily, and survival data were recorded for each group. Kaplan-Meier survival curves were plotted to compare survival rates across the treatment groups, with NanoSTING, Oseltamivir, and PBS treatment arms. The median survival was calculated.

4.10. Viral titers

On Day 20, viral titers were measured in lung samples collected from the surviving mice. Lung tissue samples from mice were homogenized using a bead mill homogenizer in minimum essential medium. Homogenized tissue samples were serially diluted in a test medium, and the virus was quantified using an endpoint dilution assay on MDCK [Madin-Darby canine kidney- MDCK cells (ATCC®, CCL-34)] cells for influenza virus. A 50 % cell culture infectious dose was determined using the Reed-Muench equation (REED et al., 1938).

4.11. Histopathology

Lungs of the mice were fixed in 10 % neutral buffered formalin, processed, paraffin-embedded, and 4-μm sections were stained with hematoxylin and eosin. Histopathological analysis was conducted to evaluate inflammation and any structural changes in lung architecture. We used an integrated scoring rubric to evaluate the pathology score (Nambulli et al., 2021). The published scoring method was modified from a 0–3 to a 0–4 score with 1 = 1–25 %; 2 = 26–50 %; 3 = 51–75 %; and 4 = 76–100 %. The original histologic criteria comprised of three compartments: airways, blood vessels, and interstitium. The sum of all three scores was reported as the cumulative lung injury score for an animal, ranging from 0 to 12. This scoring also takes into account the degeneration/necrosis of the bronchial epithelium/alveolar epithelium. A board-certified pathologist (M.S.) evaluated the sections.

CRediT authorship contribution statement

Ankita Leekha: Writing – original draft, Methodology, Investigation, Formal analysis, Data curation. **Kate Reichel:** Writing – original draft, Validation, Investigation, Formal analysis, Data curation. **Brett Hurst:** Writing – review & editing, Supervision, Project administration, Methodology, Investigation. **Navin Varadarajan:** Writing – original draft, Supervision, Project administration, Funding acquisition, Formal analysis, Conceptualization.

Declaration of competing interest

The authors declare the following financial interests/personal relationships which may be considered as potential competing interests: NV is a co-founder of CellChorus and AuraVax Therapeutics.

Acknowledgments

This publication was supported by AuraVax Therapeutics. Schematics were created using Microsoft PowerPoint, Prism, and Biorender, all of which were accessed via full licenses. We thank Dr. Alamgir Karim for providing access to the DLS and zeta sizer, Dr. Mehmet Sen for allowing access to the NanoDrop, Dr. Manu Sebastian for help with pathology, Dr. Laurence Cooper for scientific discussions, Dr. Yvonne Lee for assistance with the manuscript draft, and the Rice Shared Equipment Authority for providing access to the NanoSight.

Appendix A. Supplementary data

Supplementary data to this article can be found online at https://doi.org/10.1016/j.antiviral.2026.106342.

Data availability

Data will be made available on request.

References

Ablasser, A., et al., 2013. cGAS produces a 2'-5'-linked cyclic dinucleotide second messenger that activates STING. Nature 498, 380–384. https://doi.org/10.1038/nature12306.
Ahn, J., Barber, G.N., 2019. STING signaling and host defense against microbial infection. Exp. Mol. Med. 51, 1–10. https://doi.org/10.1038/s12276-019-0333-0.
Allen, T.M., Cullis, P.R., 2013. Liposomal drug delivery systems: from concept to clinical applications. Adv. Drug Deliv. Rev. 65, 36–48. https://doi.org/10.1016/j.addr.2012.09.037.
Allen, T.M., Martin, F.J., 2004. Advantages of liposomal delivery systems for anthracyclines. Semin. Oncol. 31, 5–15. https://doi.org/10.1053/j.seminoncol.2004.08.001.
Anderson, R., et al., 2010. Liposomal encapsulation enhances and prolongs the anti-inflammatory effects of water-soluble dexamethasone phosphate in experimental adjuvant arthritis. Arthritis Res. Ther. 12, R147. https://doi.org/10.1186/ar3089.
Andrews, N.J., et al., 2011. Predictors of immune response and reactogenicity to AS03B-adjuvanted split virion and non-adjuvanted whole virion H1N1 (2009) pandemic influenza vaccines. Vaccine 29, 7913–7919. https://doi.org/10.1016/j.vaccine.2011.08.076.
Axelsen, J.B., Yaari, R., Grenfell, B.T., Stone, L., 2014. Multiannual forecasting of seasonal influenza dynamics reveals climatic and evolutionary drivers. Proc. Natl. Acad. Sci. U. S. A. 111, 9538–9542. https://doi.org/10.1073/pnas.1321656111.
Batool, S., Chokkakula, S., Song, M.S., 2023. Influenza treatment: limitations of antiviral therapy and advantages of drug combination therapy. Microorganisms 11. https://doi.org/10.3390/microorganisms11010183.
Blest, H.T.W., Chauveau, L., 2023. cGAMP the travelling messenger. Front. Immunol. 14, 1150705. https://doi.org/10.3389/fimmu.2023.1150705.
Calzas, C., Chevalier, C., 2019. Innovative mucosal vaccine formulations against influenza A virus infections. Front. Immunol. 10, 1605. https://doi.org/10.3389/fimmu.2019.01605.
Cooper, N.J., et al., 2003. Effectiveness of neuraminidase inhibitors in treatment and prevention of influenza A and B: systematic review and meta-analyses of randomised controlled trials. Bmj 326, 1235. https://doi.org/10.1136/bmj.326.7401.1235.
Davidson, S., Crotta, S., McCabe, T.M., Wack, A., 2014. Pathogenic potential of interferon αβ in acute influenza infection. Nat. Commun. 5, 3864. https://doi.org/10.1038/ncomms4864.
Du, Y., et al., 2020. Influenza a virus antagonizes type I and type II interferon responses via SOCS1-dependent ubiquitination and degradation of JAK1. Virol. J. 17, 74. https://doi.org/10.1186/s12985-020-01348-4.
Dutkowski, R., 2010. Oseltamivir in seasonal influenza: cumulative experience in low- and high-risk patients. J. Antimicrob. Chemother. 65 (Suppl. 2), ii11–ii24. https://doi.org/10.1093/jac/dkq012.
Fomin, I., et al., 2006. Vaccination against influenza in rheumatoid arthritis: the effect of disease modifying drugs, including TNF alpha blockers. Ann. Rheum. Dis. 65, 191–194. https://doi.org/10.1136/ard.2005.036434.
Gajewski, T.F., Corrales, L., 2015. New perspectives on type I IFNs in cancer. Cytokine Growth Factor Rev. 26, 175–178. https://doi.org/10.1016/j.cytogfr.2015.01.001.
Gao, Y., et al., 2024. Antivirals for treatment of severe influenza: a systematic review and network meta-analysis of randomised controlled trials. Lancet 404, 753–763. https://doi.org/10.1016/S0140-6736(24)01307-2.
Garcia, G., et al., 2023. Innate immune pathway modulator screen identifies STING pathway activation as a strategy to inhibit multiple families of arbo and respiratory viruses. Cell Rep. Med. 4, 101024. https://doi.org/10.1016/j.xcrm.2023.101024.
Guo, J., et al., 2024. Real-world effectiveness of seasonal influenza vaccination and age as effect modifier: a systematic review, meta-analysis and meta-regression of test-negative design studies. Vaccine 42, 1883–1891. https://doi.org/10.1016/j.vaccine.2024.02.059.

Hayden, F.G., et al., 2018. Baloxavir marboxil for uncomplicated influenza in adults and adolescents. N. Engl. J. Med. 379, 913–923. https://doi.org/10.1056/NEJMoa1716197.
He, G., Massarella, J., Ward, P., 1999. Clinical pharmacokinetics of the prodrug oseltamivir and its active metabolite Ro 64-0802. Clin. Pharmacokinet. 37, 471–484. https://doi.org/10.2165/00003088-199937060-00003.
Hemann, E.A., et al., 2019. Interferon-lambda modulates dendritic cells to facilitate T cell immunity during infection with influenza A virus. Nat. Immunol. 20, 1035–1045. https://doi.org/10.1038/s41590-019-0408-z.
Holm, C.K., et al., 2016. Influenza A virus targets a cGAS-independent STING pathway that controls enveloped RNA viruses. Nat. Commun. 7, 10680. https://doi.org/10.1038/ncomms10680.
Hurt, A.C., Kelly, H., 2016. Debate regarding oseltamivir use for seasonal and pandemic influenza. Emerg. Infect. Dis. 22, 949–955. https://doi.org/10.3201/eid2206.151037.
Ishikawa, H., Ma, Z., Barber, G.N., 2009. STING regulates intracellular DNA-mediated, type I interferon-dependent innate immunity. Nature 461, 788–792. https://doi.org/10.1038/nature08476.
Killip, M.J., Fodor, E., Randall, R.E., 2015. Influenza virus activation of the interferon system. Virus Res. 209, 11–22. https://doi.org/10.1016/j.virusres.2015.02.003.
Kode, S.S., et al., 2019. A novel I117T substitution in neuraminidase of highly pathogenic avian influenza H5N1 virus conferring reduced susceptibility to oseltamivir and zanamivir. Vet. Microbiol. 235, 21–24. https://doi.org/10.1016/j.vetmic.2019.06.005.
Krammer, F., et al., 2018. Influenza. Nat. Rev. Dis. Primers 4 (3). https://doi.org/10.1038/s41572-018-0002-y.
Kumar, V., Bauer, C., Stewart, J.H.t., 2023. Targeting cGAS/STING signaling-mediated myeloid immune cell dysfunction in TIME. J. Biomed. Sci. 30, 48. https://doi.org/10.1186/s12929-023-00942-2.
Kunisaki, K.M., Janoff, E.N., 2009. Influenza in immunosuppressed populations: a review of infection frequency, morbidity, mortality, and vaccine responses. Lancet Infect. Dis. 9, 493–504. https://doi.org/10.1016/s1473-3099(09)70175-6.
Lauf, T., et al., 2024. Age-related STING suppression in macrophages contributes to increased viral load during influenza a virus infection. Immun. Ageing 21, 80. https://doi.org/10.1186/s12979-024-00482-9.
Leekha, A., et al., 2024a. An intranasal nanoparticle STING agonist protects against respiratory viruses in animal models. Nat. Commun. 15, 6053. https://doi.org/10.1038/s41467-024-50234-y.
Leekha, A., et al., 2024b. Multi-antigen intranasal vaccine protects against challenge with sarbecoviruses and prevents transmission in hamsters. Nat. Commun. 15, 6193. https://doi.org/10.1038/s41467-024-50133-2.
Leekha, A., et al., 2024c. An intranasal nanoparticle STING agonist protects against respiratory viruses in animal models. Nat. Commun. 15, 6053. https://doi.org/10.1038/s41467-024-50234-y.
Li, W., Moltedo, B., Moran, T.M., 2012. Type I interferon induction during influenza virus infection increases susceptibility to secondary Streptococcus pneumoniae infection by negative regulation of γδ T cells. J. Virol. 86, 12304–12312. https://doi.org/10.1128/jvi.01269-12.
Li, L., et al., 2014. Hydrolysis of 2'3'-cGAMP by ENPP1 and design of nonhydrolyzable analogs. Nat. Chem. Biol. 10, 1043–1048. https://doi.org/10.1038/nchembio.1661.
Liu, P., Chen, G., Zhang, J., 2022. A review of liposomes as a drug delivery system: current status of approved products, regulatory environments, and future perspectives. Molecules 27. https://doi.org/10.3390/molecules27041372.
Liu, Z., et al., 2023. Immunosenescence: molecular mechanisms and diseases. Signal Transduct. Targeted Ther. 8, 200. https://doi.org/10.1038/s41392-023-01451-2.
Luteijn, R.D., et al., 2019. SLC19A1 transports immunoreactive cyclic dinucleotides. Nature 573, 434–438. https://doi.org/10.1038/s41586-019-1553-0.
Memoli, M.J., et al., 2014. The natural history of influenza infection in the severely immunocompromised vs nonimmunocompromised hosts. Clin. Infect. Dis. 58, 214–224. https://doi.org/10.1093/cid/cit725.
Moscona, A., 2009. Global transmission of oseltamivir-resistant influenza. N. Engl. J. Med. 360, 953–956. https://doi.org/10.1056/NEJMp0900648.
Nambulli, S., et al., 2021. Inhalable Nanobody (PiN-21) prevents and treats SARS-CoV-2 infections in Syrian hamsters at ultra-low doses. Sci. Adv. 7. https://doi.org/10.1126/sciadv.abh0319.
Near, A.M., Tse, J., Young-Xu, Y., Hong, D.K., Reyes, C.M., 2022. Burden of influenza hospitalization among high-risk groups in the United States. BMC Health Serv. Res. 22, 1209. https://doi.org/10.1186/s12913-022-08586-y.
O'Hanlon, R., Shaw, M.L., 2019. Baloxavir marboxil: the new influenza drug on the market. Curr. Opin. Virol. 35, 14–18. https://doi.org/10.1016/j.coviro.2019.01.006.
Organization, W. H. Burden of disease, <https://www.who.int/teams/global-influenza-programme/surveillance-and-monitoring/burden-of-disease>(n.d.).
Osterholm, M.T., Kelley, N.S., Sommer, A., Belongia, E.A., 2012. Efficacy and effectiveness of influenza vaccines: a systematic review and meta-analysis. Lancet Infect. Dis. 12, 36–44. https://doi.org/10.1016/S1473-3099(11)70295-X.
Peteranderl, C., Herold, S., Schmoldt, C., 2016. Human influenza virus infections. Semin. Respir. Crit. Care Med. 37, 487–500. https://doi.org/10.1055/s-0036-1584801.
Petrova, V.N., Russell, C.A., 2018. The evolution of seasonal influenza viruses. Nat. Rev. Microbiol. 16, 47–60. https://doi.org/10.1038/nrmicro.2017.118.
Pöpperl, P., Stoff, M., Beineke, A., 2025. Alveolar macrophages in viral respiratory infections: sentinels and saboteurs of lung defense. Int. J. Mol. Sci. 26. https://doi.org/10.3390/ijms26010407.
Qiu, S., Shen, Y., Pan, H., Wang, J., Zhang, Q., 2015. Effectiveness and safety of oseltamivir for treating influenza: an updated meta-analysis of clinical trials. Infect. Dis. (Lond.) 47, 808–819. https://doi.org/10.3109/23744235.2015.1067369.
Reed, L.J., Muench, H.A., 1938. Simple method of estimating fifty per cent ENDPOINTS12. Am. J. Epidemiol. 27, 493–497. https://doi.org/10.1093/oxfordjournals.aje.a118408.
Ritchie, C., Cordova, A.F., Hess, G.T., Bassik, M.C., Li, L., 2019. SLC19A1 is an importer of the immunotransmitter cGAMP. Mol. Cell 75, 372–381 e375. https://doi.org/10.1016/j.molcel.2019.05.006.
Webby, R.J., Uyeki, T.M., 2024. An update on highly pathogenic avian influenza A (H5N1) virus, clade 2.3.4.4b. J. Infect. Dis. 230, 533–542. https://doi.org/10.1093/infdis/jiae379.
Wu, W., Metcalf, J.P., 2020. The role of type I IFNs in influenza: antiviral superheroes or immunopathogenic villains? J. Innate Immun. 12, 437–447. https://doi.org/10.1159/000508379.
Yen, H.L., Monto, A.S., Webster, R.G., Govorkova, E.A., 2005. Virulence may determine the necessary duration and dosage of oseltamivir treatment for highly pathogenic A/Vietnam/1203/04 influenza virus in mice. J. Infect. Dis. 192, 665–672. https://doi.org/10.1086/432008.
Yu, X., Cai, L., Yao, J., Li, C., Wang, X., 2024. Agonists and inhibitors of the cGAS-STING pathway. Molecules 29. https://doi.org/10.3390/molecules29133121.
Zheng, B.J., et al., 2008. Delayed antiviral plus immunomodulator treatment still reduces mortality in mice infected by high inoculum of influenza A/H5N1 virus. Proc. Natl. Acad. Sci. U. S. A. 105, 8091–8096. https://doi.org/10.1073/pnas.0711942105.
Zidar, D.A., et al., 2019. Association of lymphopenia with risk of mortality among adults in the US general population. JAMA Netw. Open 2, e1916526. https://doi.org/10.1001/jamanetworkopen.2019.16526.